Eur. Phys. J. C (2020) 80:365
https://doi.org/10.1140/epjc/s10052-020-7940-8

THE EUROPEAN PHYSICAL JOURNAL C

Regular Article - Theoretical Physics

Revisiting the B-physics anomalies in R-parity violating MSSM

Quan-Yi Hu[1,a], **Ya-Dong Yang**[2,b], **Min-Di Zheng**[2,c]

[1] School of Physics and Electrical Engineering, Anyang Normal University, Anyang 455000, Henan, China
[2] Institute of Particle Physics and Key Laboratory of Quark and Lepton Physics (MOE), Central China Normal University, Wuhan 430079, Hubei, China

Received: 4 March 2020 / Accepted: 15 April 2020 / Published online: 6 May 2020

Abstract In recent years, several deviations from the Standard Model predictions in semileptonic decays of B-meson might suggest the existence of new physics which would break the lepton-flavour universality. In this work, we have explored the possibility of using muon sneutrinos and right-handed sbottoms to solve these B-physics anomalies simultaneously in R-parity violating minimal supersymmetric standard model. We find that the photonic penguin induced by exchanging sneutrino can provide sizable lepton flavour universal contribution due to the existence of logarithmic enhancement for the first time. This prompts us to use the two-parameter scenario $(C_9^{\rm V}, C_9^{\rm U})$ to explain $b \to s\ell^+\ell^-$ anomaly. Finally, the numerical analyses show that the muon sneutrinos and right-handed sbottoms can explain $b \to s\ell^+\ell^-$ and $R(D^{(*)})$ anomalies simultaneously, and satisfy the constraints of other related processes, such as $B \to K^{(*)}\nu\bar{\nu}$ decays, $B_s - \bar{B}_s$ mixing, Z decays, as well as $D^0 \to \mu^+\mu^-$, $\tau \to \mu\rho^0$, $B \to \tau\nu$, $D_s \to \tau\nu$, $\tau \to K\nu$, $\tau \to \mu\gamma$, and $\tau \to \mu\mu\mu$ decays.

1 Introduction

Recently, several flavour anomalies in semileptonic B-decays have been reported, which have been attracting great interest. Among them, the observables $R_{K^{(*)}} = \mathcal{B}(B \to K^{(*)}\mu^+\mu^-)/\mathcal{B}(B \to K^{(*)}e^+e^-)$ in flavour-changing neutral current $b \to s\ell^+\ell^-$ ($\ell = e, \mu$) transition and the observables $R(D^{(*)}) = \mathcal{B}(B \to D^{(*)}\tau\nu)/\mathcal{B}(B \to D^{(*)}\ell\nu)$ in flavour-changing charged current $b \to c\tau\nu$ transition are particularly striking. The advantage of considering the ratios $R_{K^{(*)}}$ and $R(D^{(*)})$ instead of the branching fractions themselves is that, apart from the significant reduction of the experimental systematic uncertainties, the Cabibbo–Kobayashi–Maskawa (CKM) matrix elements cancel out and the dependence on the transition form factors become much weaker. These observables can be good probes to test the lepton-flavour universality (LFU) held in the Standard Model (SM).

[a] e-mail: qyhu@aynu.edu.cn (corresponding author)
[b] e-mail: yangyd@mail.ccnu.edu.cn
[c] e-mail: zhengmindi@mails.ccnu.edu.cn

The latest measurement of R_K by LHCb collaboration gives [1,2]

$$R_K = 0.846^{+0.060+0.016}_{-0.054-0.014}, \; 1.1 < q^2 < 6\,\text{GeV}^2, \tag{1}$$

but the SM prediction is around 1 with $\mathcal{O}(1\%)$ uncertainty [3], there is 2.5σ discrepancy. Moreover, the measurement of R_{K^*} by LHCb at low and high q^2 are [4]

$$R_{K^*} = \begin{cases} 0.66^{+0.11}_{-0.07} \pm 0.03, & 0.045 < q^2 < 1.1\,\text{GeV}^2 \\ 0.69^{+0.11}_{-0.07} \pm 0.05, & 1.1 < q^2 < 6.0\,\text{GeV}^2 \end{cases}, \tag{2}$$

while the SM predictions are $R_{K^*}^{[0.045,\,1.1]} = 0.906 \pm 0.028$ and $R_{K^*}^{[1.1,\,6.0]} = 1.00 \pm 0.01$ [3]. The measurements show 2.1σ discrepancy in the low q^2 region and 2.5σ discrepancy in the high q^2 region, respectively. The Belle collaboration also reported their measurements of $R_{K^{(*)}}$ [5,6], which are consistent with the SM predictions within their quite large error bars. In addition to $R_{K^{(*)}}$, there are also some other deviations in $b \to s\mu^+\mu^-$ transition, such as the angular observable P_5' [7–9] of $B \to K^*\mu^+\mu^-$ decay with 2.6σ discrepancy [10–15] and the differential branching fraction of $B_s \to \phi\mu^+\mu^-$ decay with 3.3σ discrepancy [16,17].

These deviations indicate the possible existence of new physics (NP) beyond the SM in $b \to s\ell^+\ell^-$ transition. This NP may break LFU. Many recent model-independent analyses [18–25] show that some scenarios can explain the $b \to s\ell^+\ell^-$ anomaly well. To express the fit results, we consider the low-energy effective weak Lagrangian governing the $b \to s\ell^+\ell^-$ transition

$$\mathcal{L}_{\rm eff} = \frac{4G_F}{\sqrt{2}}\eta_t \sum_i C_i \mathcal{O}_i + {\rm H.c.}, \quad (3)$$

where CKM factor $\eta_t \equiv V_{tb}V_{ts}^*$. We mainly concern the semileptonic operators

$$\mathcal{O}_9 = \frac{e^2}{16\pi^2}(\bar{s}\gamma_\mu P_L b)(\bar{\ell}\gamma^\mu \ell), \quad (4)$$
$$\mathcal{O}_{10} = \frac{e^2}{16\pi^2}(\bar{s}\gamma_\mu P_L b)(\bar{\ell}\gamma^\mu \gamma_5 \ell), \quad (5)$$

where $P_L = (1-\gamma_5)/2$ is the left-handed chirality projector. The Wilson coefficients $C_{9,10} = C_{9,10}^{\rm SM} + C_{9,10}^{\rm NP}$. In this work, we try to explain the anomaly through a two-parameter scenario where the total NP effects are given by [26]

$$C_{9,\mu}^{\rm NP} = C_9^{\rm V} + C_9^{\rm U}, \quad C_{10,\mu}^{\rm NP} = -C_9^{\rm V}, \quad (6)$$
$$C_{9,e}^{\rm NP} = C_9^{\rm U}, \quad C_{10,e}^{\rm NP} = 0. \quad (7)$$

The global analyses show that this scenario has the largest pull-value. The best-fit point performed by Ref. [20] is $(C_9^{\rm V}, C_9^{\rm U}) = (-0.30, -0.74)$, with the 2σ range being

$$-0.53 < C_9^{\rm V} < -0.10, \quad -1.15 < C_9^{\rm U} < -0.25. \quad (8)$$

As we will see in the following discussion, this scenario can be implemented naturally in the R-parity violating minimal supersymmetric standard model (MSSM) [27].

The combined measurements of $R(D^*)$ and $R(D)$ are from BaBar [28,29] and Belle [30,31], and Belle [32,33] and LHCb [34–36] only give the measurements of $R(D^*)$. After being averaged by the Heavy Flavor Averaging Group (HFLAV) [37], they give the results as follows [38]

$$R(D)_{\rm avg} = 0.340 \pm 0.027 \pm 0.013, \quad (9)$$
$$R(D^*)_{\rm avg} = 0.295 \pm 0.011 \pm 0.008, \quad (10)$$

with a correlation of -0.38. Comparing these with the arithmetic average of the SM predictions [38–42],

$$R(D)_{\rm SM} = 0.299 \pm 0.003, \quad R(D^*)_{\rm SM} = 0.258 \pm 0.005, \quad (11)$$

one can see that the difference between experiment and theory is at about 3.08σ, implying the existence of LFU violating NP in the charged-current B-decays. Global analyses [43–47] show that the NP contributing to the left-handed operator $(\bar{c}\gamma_\mu P_L b)(\bar{\tau}\gamma^\mu P_L \nu)$ can solve the $R(D^{(*)})$ anomaly. Such operator can be generated in R-parity violating MSSM by exchanging the right-handed down type squarks at tree level.

There have been attempts to explain the $b \to s\ell^+\ell^-$ anomaly [48–52] or $R(D^{(*)})$ anomaly [53–57] or both of them [58–60] by R-parity violating interactions in the supersymmetric (SUSY) models. For example, based on the inspiration from the paper by Bauer and Neubert [61], the authors in Ref. [58] investigated the possibility of using right-handed down type squarks to explain the $b \to s\ell^+\ell^-$ and $R(D^{(*)})$ anomalies simultaneously, and found that this was impossible due to the severe constraints from $B \to K^{(*)}\nu\bar{\nu}$ decays. Considering that the parameter space obtained by using squarks to explain $b \to s\ell^+\ell^-$ anomaly is very small [49,50,58] due to the strict constraints from other related processes, such as $B \to K^{(*)}\nu\bar{\nu}$ decays and $B_s - \bar{B}_s$ mixing, the authors in Ref. [52] used sneutrinos to explain it and found that it is almost unconstrained by other related processes. Based on this knowledge, in this work, we will explore the possibility of using muon sneutrinos $\tilde{\nu}_\mu$ and right-handed sbottoms $\tilde{b}_R$ to explain the $b \to s\ell^+\ell^-$ and $R(D^{(*)})$ anomalies simultaneously within the context of R-parity violating MSSM.

Our paper is organized as follows. In Sect. 2, we scrutinize all the one-loop contributions of terms $\lambda'_{ijk}L_iQ_jD_k^c$ to $b \to s\ell^+\ell^-$ processes in the framework of R-parity violating MSSM, and then give our scenario to explain the $b \to s\ell^+\ell^-$ anomaly. Discussions of $R(D^{(*)})$ anomaly and other related processes are included in Sect. 3. The numerical analyses and results are shown in Sect. 4. Our conclusions are finally made in Sect. 5.

2 $b \to s\ell^+\ell^-$ processes in R-parity violating MSSM

The superpotential terms violating R-parity in the MSSM are [27]

$$W_{\rm RPV} = \mu_i L_i H_u + \frac{1}{2}\lambda_{ijk}L_iL_jE_k^c + \lambda'_{ijk}L_iQ_jD_k^c + \frac{1}{2}\lambda''_{ijk}U_i^cD_j^cD_k^c, \quad (12)$$

where the generation indices are denoted by $i, j, k = 1, 2, 3$ and the colour indices are suppressed. All repeated indices are assumed to be summed over throughout this paper unless otherwise stated (For example, repeated indices in both numerator and denominator are not automatically summed). H_u, L and Q are $SU(2)$ doublet chiral superfields while E^c, D^c and U^c are $SU(2)$ singlet chiral superfields.

In this work, we are mainly interested in the terms $\lambda'_{ijk}L_iQ_jD_k^c$ which related to both quarks and leptons. This choice can also alleviate the constraint of sneutrino masses on the collider, because the lower limit of sneutrino masses will be as high as TeV scale [62–65] when there are non-zero λ and λ' at the same time. The corresponding Lagrangian can be obtained by the chiral superfields composing of the fermions and sfermions as follows

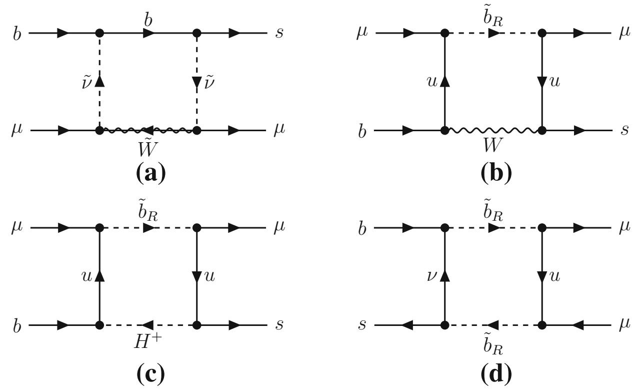

Fig. 1 Box diagrams for $b \to s\mu^+\mu^-$ transition in our scenario. **a** Shows an example $\tilde{W} - b$ box diagram, **b** shows an example $W - \tilde{b}_R$ box diagram, **c** shows the $H^\pm - \tilde{b}_R$ box diagram, and **d** shows an example $4\lambda'$ box diagram

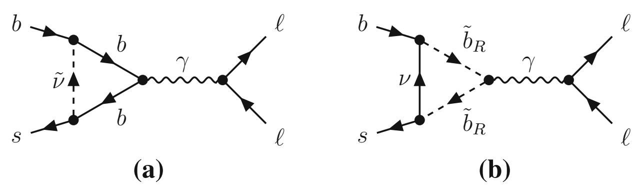

Fig. 2 Photonic penguin diagrams studied in our scenario

$$\mathcal{L} = \lambda'_{ijk}\big(\tilde{\nu}_{Li}\bar{d}_{Rk}d_{Lj} + \tilde{d}_{Lj}\bar{d}_{Rk}\nu_{Li} + \tilde{d}^*_{Rk}\bar{\nu}^c_{Li}d_{Lj} - \tilde{l}_{Li}\bar{d}_{Rk}u_{Lj} - \tilde{u}_{Lj}\bar{d}_{Rk}l_{Li} - \tilde{d}^*_{Rk}\bar{l}^c_{Li}u_{Lj}\big) + \text{H.c.}, \quad (13)$$

where the sparticles are denoted by "~", and "c" indicates charge conjugated fields. Working in the mass eigenstates for the down type quarks and assuming sfermions are in their mass eigenstates, one replaces u_{Lj} by $(V^\dagger u_L)_j$ in Eq. (13).

These R-parity violating interactions can induce $b \to s\ell^+\ell^-$ processes by exchanging left-handed up squarks $\tilde{u}_{Lj}$ at tree level, but resulting in the operators with right-handed quark current, which are unable to explain the $b \to s\ell^+\ell^-$ anomaly. This unwanted effect can be eliminated by assuming that the masses of $\tilde{u}_{Lj}$ are very large or/and by assuming that $\lambda'_{ij2} = 0$. Assuming that $\lambda'_{ij2} = 0$ also forbids the exchange of $\tilde{l}_{Li}$ or/and $\tilde{d}_{Lj}$ in one loop level to affect the $b \to s\ell^+\ell^-$ processes.[1] In the following discussion, we should assume that $\lambda'_{ij1} = \lambda'_{ij2} = 0$.

Next, we will show the contributions of R-parity violating MSSM to $b \to s\ell^+\ell^-$ processes. All the Feynman diagrams include four $\tilde{W} - b$ box diagrams (Fig. 1a), five $W - \tilde{b}_R$ box diagrams (one of which is Goldstone$-\tilde{b}_R$ box diagram) (Fig. 1b), one $H^\pm - \tilde{b}_R$ box diagram (Fig. 1c), two $4\lambda'$ box diagrams (Fig. 1d) and two γ-penguin diagrams (Fig. 2). Most of these results can be found in Refs. [49,50,52,58], however, to our knowledge, the results of the diagram induced by exchanging charged Higgs $H^\pm$ and right-handed sbottom $\tilde{b}_R$ in loop are the first to be given in this paper. The photonic penguin diagrams, which have been neglected in previous work, play an important role in our discussion, as we will explain in more detail later. We do not find sizable Z-penguin contributions to $b \to s\ell^+\ell^-$ processes. In this work, the contributions of γ/Z-penguin diagrams always include their supersymmetric counterparts unless otherwise specified. For convenience, the following Passarino–Veltman functions [67] D_0 and D_2 are defined as

$$\begin{aligned}
&D_0[m_1^2, m_2^2, m_3^2, m_4^2] \\
&\equiv \int \frac{d^4k}{(2\pi)^4}\frac{1}{(k^2-m_1^2)(k^2-m_2^2)(k^2-m_3^2)(k^2-m_4^2)} \\
&= -\frac{i}{16\pi^2}\Bigg[\frac{m_1^2\log(m_1^2)}{(m_1^2-m_2^2)(m_1^2-m_3^2)(m_1^2-m_4^2)} \\
&\quad + (m_1 \leftrightarrow m_2) + (m_1 \leftrightarrow m_3) + (m_1 \leftrightarrow m_4)\Bigg], \qquad (14)
\end{aligned}$$

$$\begin{aligned}
&D_2[m_1^2, m_2^2, m_3^2, m_4^2] \\
&\equiv \int \frac{d^4k}{(2\pi)^4}\frac{k^2}{(k^2-m_1^2)(k^2-m_2^2)(k^2-m_3^2)(k^2-m_4^2)} \\
&= -\frac{i}{16\pi^2}\Bigg[\frac{m_1^4\log(m_1^2)}{(m_1^2-m_2^2)(m_1^2-m_3^2)(m_1^2-m_4^2)} \\
&\quad + (m_1 \leftrightarrow m_2) + (m_1 \leftrightarrow m_3) + (m_1 \leftrightarrow m_4)\Bigg]. \qquad (15)
\end{aligned}$$

The contributions of box diagram are listed below. We eliminate the contributions of all box diagrams to $b \to se^+e^-$ processes by assuming $\lambda'_{1j3} = 0$.

- The contributions of $\tilde{W} - b$ box diagram to $b \to s\mu^+\mu^-$ processes are given by

$$\begin{aligned}
C_9^{\mathrm{V}(\tilde{W})} = &\frac{-i\pi^2}{\sqrt{2}G_F\sin^2\theta_W\eta_t} \\
&\times \Big(\lambda'_{2i3}\lambda'^*_{223}V_{ib}D_2[m^2_{\tilde{W}}, m^2_{\tilde{u}_{Li}}, m^2_{\tilde{\nu}_\mu}, m_b^2] \\
&- \lambda'_{2i3}\lambda'^*_{2j3}V_{ib}V^*_{js}D_2[m^2_{\tilde{W}}, m^2_{\tilde{u}_{Li}}, m^2_{\tilde{u}_{Lj}}, m_b^2] \\
&+ \lambda'_{233}\lambda'^*_{2j3}V^*_{js}D_2[m^2_{\tilde{W}}, m^2_{\tilde{u}_{Lj}}, m^2_{\tilde{\nu}_\mu}, m_b^2] \\
&- \lambda'_{233}\lambda'^*_{223}D_2[m^2_{\tilde{W}}, m^2_{\tilde{\nu}_\mu}, m^2_{\tilde{\nu}_\mu}, m_b^2]\Big), \qquad (16)
\end{aligned}$$

where the winos engage these interactions with left-hand up type squarks and muon sneutrinos. The last term plays an important role in numerical analysis [52].

[1] In this work, we don't consider contributions only from R-parity conserving MSSM, because these contributions can be ignored numerically [66].

- The contributions of $W-\tilde{b}_R$ box diagram to $b \to s\mu^+\mu^-$ processes are given by

$$C_9^{\mathrm{V}(W)} = \frac{-i\pi^2}{\sqrt{2}G_F \sin^2\theta_W \eta_t} \times \Big(\tilde{\lambda}'_{2i3}\lambda'^*_{223} V_{ib} D_2[m^2_{\tilde{b}_R}, m^2_{u_i}, m^2_W, 0] - \tilde{\lambda}'_{2i3}\tilde{\lambda}'^*_{2j3} V_{ib} V^*_{js} D_2[m^2_{\tilde{b}_R}, m^2_{u_i}, m^2_{u_j}, m^2_W] + \lambda'_{233}\tilde{\lambda}'^*_{2j3} V^*_{js} D_2[m^2_{\tilde{b}_R}, m^2_{u_j}, m^2_W, 0] - \lambda'_{233}\lambda'^*_{223} D_2[m^2_{\tilde{b}_R}, m^2_W, 0, 0] + \tilde{\lambda}'_{2i3}\tilde{\lambda}'^*_{2j3} V_{ib} V^*_{js} \frac{m^2_{u_i} m^2_{u_j}}{m^2_W} \times D_0[m^2_{\tilde{b}_R}, m^2_{u_i}, m^2_{u_j}, m^2_W]\Big), \tag{17}$$

where $\tilde{\lambda}'_{ijk} \equiv \lambda'_{ilk} V^*_{jl}$. The right-hand sbottom $\tilde{b}_R$ is the only NP particle here. In the limit $m_{\tilde{b}_R} \gg m_t$, one has $C_9^{\mathrm{V}(W)} = \frac{m_t^2}{16\pi\alpha m^2_{\tilde{b}_R}} |\lambda'_{233}|^2$ [49,50,61] which is obviously positive.
- The contributions of $H^\pm - \tilde{b}_R$ box diagram to $b \to s\mu^+\mu^-$ processes are given by

$$C_9^{\mathrm{V}(H^\pm)} = \frac{-i\pi^2 V_{ib} V^*_{js} \tilde{\lambda}'_{2i3}\tilde{\lambda}'^*_{2j3}}{\sqrt{2}G_F \sin^2\theta_W \tan^2\beta \eta_t} \frac{m^2_{u_i} m^2_{u_j}}{m^2_W} \times D_0[m^2_{H^\pm}, m^2_{u_i}, m^2_{u_j}, m^2_{\tilde{b}_R}], \tag{18}$$

which should be considered in the following numerical analysis. The $\tan\beta = v_u/v_d$ where v_u and v_d are the vacuum expectation values of two Higgs doublets respectively.
- The contributions of $4\lambda'$ box diagram to $b \to s\mu^+\mu^-$ processes are given by

$$C_9^{\mathrm{V}(4\lambda')} = \frac{-i\pi\lambda'_{i33}\lambda'^*_{i23}}{4\sqrt{2}G_F\alpha\eta_t} \Big(|\tilde{\lambda}'_{2j3}|^2 D_2[m^2_{\tilde{b}_R}, m^2_{\tilde{b}_R}, m^2_{u_j}, 0] + |\lambda'_{2j3}|^2 D_2[m^2_{\tilde{u}_{Lj}}, m^2_{\tilde{\nu}_i}, m^2_b, m^2_b]\Big). \tag{19}$$

The contributions of photonic penguin diagrams are lepton flavour universal which naturally gives us a nonzero C_9^{U}

$$C_9^{\mathrm{U}} = \frac{\sqrt{2}\lambda'_{i33}\lambda'^*_{i23}}{36 G_F \eta_t}\left[\frac{1}{6m^2_{\tilde{b}_R}} - \left(\frac{4}{3} + \log\frac{m_b^2}{m^2_{\tilde{\nu}_i}}\right)\frac{1}{m^2_{\tilde{\nu}_i}}\right]. \tag{20}$$

As stated in Ref. [52], this result is consistent with that in Ref. [68], but it has a *negative* sign different from that in Ref. [50]. The first term in Eq. (20) comes from the contribution of Fig. 2b, like the photonic penguin induced by scalar leptoquark. We find this term gives a negligible contribution, which is in agreement with Refs. [61,69]. However the second term in Eq. (20) has a significant contribution because of the logarithmic enhancement, which has never been addressed before. These photonic penguins also contribute new electromagnetic dipole operator $\mathcal{O}_7 = \frac{m_b}{e}(\bar{s}\sigma^{\alpha\beta}P_R b)F_{\alpha\beta}$, which is strictly constrained by $B \to X_s\gamma$ decay [9]. Fortunately, we find that the corresponding contribution can be ignored numerically because there such logarithmic enhancement is absent [50,52,68].

We will discuss the possibility of using muon sneutrinos $\tilde{\nu}_\mu$ and right-handed sbottoms $\tilde{b}_R$ to explain $b \to s\ell^+\ell^-$ anomaly, for which we set the mass of tau sneutrinos $\tilde{\nu}_\tau$ and three left-handed up type squarks $\tilde{u}_{Lj}$ sufficiently large that the contributions of the loop diagrams containing them are ignored.[2] The contribution from $H^\pm - \tilde{b}_R$ box diagram is usually positive, and we find that it is numerically negligible when $\tan\beta > 2$. Thus, the contributions to only muon channel are

$$C_9^{\mathrm{V}} = -\frac{\sqrt{2}\lambda'_{233}\lambda'^*_{223} f(x_{\tilde{\nu}_\mu})}{32 G_F \sin^2\theta_W \eta_t m^2_{\tilde{\nu}_\mu}} + \frac{|\lambda'_{233}|^2 x_{\tilde{b}_R}}{16\pi\alpha} - \frac{\lambda'_{i33}\lambda'^*_{i23}\left[|\tilde{\lambda}'_{213}|^2 + |\tilde{\lambda}'_{223}|^2 - |\tilde{\lambda}'_{233}|^2 f\left(1/x_{\tilde{b}_R}\right)\right]}{64\sqrt{2}\pi G_F \alpha\eta_t m^2_{\tilde{b}_R}}, \tag{21}$$

where $x_{\tilde{\nu}_\mu} \equiv m^2_{\tilde{\nu}_\mu}/m^2_{\tilde{W}}$, $x_{\tilde{b}_R} \equiv m_t^2/m^2_{\tilde{b}_R}$, and the loop function $f(x) \equiv \frac{x(1-x+\log x)}{(1-x)^2}$.

3 $R(D^{(*)})$ anomaly and other constraints

In this section, we discuss the interpretation of $R(D^{(*)})$ anomaly and consider the constraints imposed by other related processes from B, D, K, τ, and Z decays.

3.1 $R(D^{(*)})$ anomaly

In R-parity violating MSSM, the charged current processes $d_j \to u_n l_l \nu_i$ are induced by exchanging $\tilde{b}_R$ at tree level. The effective Lagrangian of these processes are given by

$$\mathcal{L}_{\mathrm{eff}} = -\frac{4G_F}{\sqrt{2}} V_{nj}(\delta_{li} + C_{njli})\bar{u}_n\gamma_\mu P_L d_j \bar{l}_l\gamma^\mu P_L \nu_i + \text{H.c.}, \tag{22}$$

[2] In our numerical analysis, we find that the contribution of the loop diagrams containing $\tilde{\nu}_\tau$ is numerically negligible when the mass of $\tilde{\nu}_\tau$ is a few TeV or larger. The same conclusion is true for $\tilde{u}_L$ where the mass of $\tilde{u}_L$ is a few 10 TeV or larger. Here, we consider that $m_{\tilde{\nu}_\mu} < m_{\tilde{\nu}_\tau}$, which can be achieved, for example, by setting the hierarchy of neutrino Yukawas $Y_{\nu_2} < Y_{\nu_3}$ in the $\mu\nu$SSM [70].

where the Wilson coefficient C_{njli} is

$$C_{njli} = \frac{\lambda'_{ij3}\tilde{\lambda}'^{*}_{ln3}}{4\sqrt{2}G_F V_{nj} m^2_{\tilde{b}_R}}. \tag{23}$$

Because taking $\lambda'_{1j3} = 0$ to eliminate the contributions of box diagrams to $b \to s e^+ e^-$ processes,[3] we have $C_{nj1i} = C_{njl1} = 0$. It is useful to define the ratio

$$R_{njl} \equiv \frac{\mathcal{B}(d_j \to u_n l_l \nu)}{\mathcal{B}(d_j \to u_n l_l \nu)_{\rm SM}} = \sum_{i=1}^{3} \left|\delta_{li} + C_{njli}\right|^2, \tag{24}$$

and we have

$$\frac{R(D)}{R(D)_{\rm SM}} = \frac{R(D^*)}{R(D^*)_{\rm SM}} = \frac{2R_{233}}{R_{232}+1}. \tag{25}$$

To obtain the allowed parameter region, we use the following best fit value in the R-parity violating scenario

$$\frac{R(D)}{R(D)_{\rm SM}} = \frac{R(D^*)}{R(D^*)_{\rm SM}} = 1.14 \pm 0.04. \tag{26}$$

3.2 Constraints from the tree-level processes

In the scenario we set up, some other processes receive tree level R-parity violating contributions. Here we mainly discuss the constraints from neutral current processes $B \to K^{(*)}\nu\bar{\nu}$, $B \to \pi\nu\bar{\nu}$, $K \to \pi\nu\bar{\nu}$, $D^0 \to \mu^+\mu^-$ and $\tau \to \mu\rho^0$, as well as charged current processes $B \to \tau\nu$, $D_s \to \tau\nu$ and $\tau \to K\nu$. These decays relate to

$$\frac{\lambda'_{ij3}\lambda'^{*}_{lm3}}{2m^2_{\tilde{b}_R}} \bar{d}_m \gamma^\mu P_L d_j \bar{\nu}_l \gamma_\mu P_L \nu_i, \tag{27}$$

$$\frac{\tilde{\lambda}'_{ij3}\tilde{\lambda}'^{*}_{lm3}}{2m^2_{\tilde{b}_R}} \bar{u}_m \gamma^\mu P_L u_j \bar{l}_l \gamma_\mu P_L l_i, \tag{28}$$

$$-\frac{\lambda'_{ij3}\tilde{\lambda}'^{*}_{lm3}}{2m^2_{\tilde{b}_R}} \bar{u}_m \gamma^\mu P_L d_j \bar{l}_l \gamma_\mu P_L \nu_i. \tag{29}$$

The effective Lagrangian for $B \to K^{(*)}\nu\bar{\nu}$, $B \to \pi\nu\bar{\nu}$ and $K \to \pi\nu\bar{\nu}$ decays are defined by

$$\mathcal{L}_{\rm eff} = (C^{\rm SM}_{mj}\delta_{li} + C^{\nu_l\bar{\nu}_i}_{mj})(\bar{d}_m \gamma^\mu P_L d_j)(\bar{\nu}_l \gamma_\mu P_L \nu_i) + {\rm H.c.}, \tag{30}$$

where [71]

$$C^{\rm SM}_{mj} = -\frac{\sqrt{2}G_F \alpha X(x_t)}{\pi \sin^2\theta_W} V_{tj} V^*_{tm}, \tag{31}$$

is the SM one. The loop function $X(x_t) \equiv \frac{x_t(x_t+2)}{8(x_t-1)} + \frac{3x_t(x_t-2)}{8(x_t-1)^2}\log(x_t)$ with $x_t \equiv m_t^2/m_W^2$. The R-parity violating contributions are given by

$$C^{\nu_l\bar{\nu}_i}_{mj} = \frac{\lambda'_{ij3}\lambda'^{*}_{lm3}}{2m^2_{\tilde{b}_R}}. \tag{32}$$

It is useful to define the ratio

$$R^{\nu\bar{\nu}}_{mj} \equiv \frac{\mathcal{B}(d_j \to d_m \nu\bar{\nu})}{\mathcal{B}(d_j \to d_m \nu\bar{\nu})_{\rm SM}} = \frac{\sum_{i=1}^{3}\left|C^{\rm SM}_{mj} + C^{\nu_i\bar{\nu}_i}_{mj}\right|^2 + \sum^{3}_{i\neq l}\left|C^{\nu_l\bar{\nu}_i}_{mj}\right|^2}{3\left|C^{\rm SM}_{mj}\right|^2}. \tag{33}$$

The upper limit of $B \to K^{(*)}\nu\bar{\nu}$ decay corresponds to $R^{\nu\bar{\nu}}_{23} < 2.7$ [71–73] at 90% confidence level (CL), and the upper limit of $B \to \pi\nu\bar{\nu}$ decay is related to $R^{\nu\bar{\nu}}_{13} < 830.5$ [74,75] at 90% CL. By combining the SM prediction $\mathcal{B}(K^+ \to \pi^+\nu\bar{\nu})_{\rm SM} = (9.24 \pm 0.83) \times 10^{-11}$ [76] with experimental measurement $\mathcal{B}(K^+ \to \pi^+\nu\bar{\nu})_{\rm exp} = (1.7 \pm 1.1) \times 10^{-10}$ [77], we obtain a stringent constraint from $K \to \pi\nu\bar{\nu}$ decay that makes

$$|\lambda'_{i23}\lambda'^{*}_{l13}| < 7.4 \times 10^{-4}(m_{\tilde{b}_R}/1\,{\rm TeV})^2. \tag{34}$$

Therefore, we will assume $\lambda'_{i1k} = 0$ to satisfy this constraint. At the same time, under this assumption, $B \to \pi\nu\bar{\nu}$ decay is unaffected by the NP.

The branching fraction for $D^0 \to \mu^+\mu^-$ decay is given by [58]

$$\mathcal{B}(D^0 \to \mu^+\mu^-) = \frac{\tau_D f_D^2 m_D m_\mu^2}{32\pi}\left|\frac{\tilde{\lambda}'_{223}\tilde{\lambda}'^{*}_{213}}{2m^2_{\tilde{b}_R}}\right|^2 \sqrt{1 - \frac{4m_\mu^2}{m_D^2}}, \tag{35}$$

where decay constant of D^0 is $f_D = 209.0 \pm 2.4$ MeV [78]. The mean life $\tau_D = 410.1 \pm 1.5$ fs [77] and the upper limit of branching fraction of $D^0 \to \mu^+\mu^-$ decay is 6.2×10^{-9} at 90% CL [77]. The corresponding constraint is $|\lambda'_{223}|^2 < 0.31(m_{\tilde{b}_R}/1\,{\rm TeV})^2$.

The branching fraction for $\tau \to \mu\rho^0$ decay is given by [79]

$$\mathcal{B}(\tau \to \mu\rho^0) = \frac{\tau_\tau f_\rho^2 m_\tau^3}{128\pi}\left|\frac{\tilde{\lambda}'_{313}\tilde{\lambda}'^{*}_{213}}{2m^2_{\tilde{b}_R}}\right|^2 \left(1 - \frac{m_\rho^2}{m_\tau^2}\right)$$

[3] In fact, by combining the assumptions $\lambda'_{1j3} = 0$ and $\lambda'_{ij1} = \lambda'_{ij2} = 0$, we can get $\lambda'_{1jk} = 0$, which implies that the contribution of box diagrams of NP to the first generation leptons and sleptons is zero, because we only consider the terms $\lambda'_{ijk} L_i Q_j D^c_k$.

$$\times\left(1+\frac{m_\rho^2}{m_\tau^2}-2\frac{m_\rho^4}{m_\tau^4}\right), \tag{36}$$

where $\tau_\tau = 290.3 \pm 0.5$ fs and the decay constant $f_\rho = 153$ MeV [50]. The current experimental upper limit on the branching fraction for this process is $\mathcal{B}(\tau \to \mu\rho^0) < 1.2 \times 10^{-8}$ at 90% CL [77]. The corresponding constraint is $|\lambda'_{323}\lambda'^*_{223}| < 0.38(m_{\tilde{b}_R}/1\,\text{TeV})^2$.

The formulas for charged current processes are given, respectively, by

$$\frac{\mathcal{B}(B\to\tau\nu)}{\mathcal{B}(B\to\tau\nu)_{\text{SM}}} = R_{133}, \tag{37}$$

$$\frac{\mathcal{B}(D_s\to\tau\nu)}{\mathcal{B}(D_s\to\tau\nu)_{\text{SM}}} = R_{223}, \tag{38}$$

$$\frac{\mathcal{B}(\tau\to K\nu)}{\mathcal{B}(\tau\to K\nu)_{\text{SM}}} = R_{123}. \tag{39}$$

The corresponding experimental and theoretical values are listed, respectively, as follows: $\mathcal{B}(B\to\tau\nu)_{\text{exp}} = (1.09 \pm 0.24)\times 10^{-4}$ [77], $\mathcal{B}(B\to\tau\nu)_{\text{SM}} = (9.47\pm 1.82)\times 10^{-5}$ [80]; $\mathcal{B}(D_s\to\tau\nu)_{\text{exp}} = (5.48\pm0.23)\%$ [77], $\mathcal{B}(D_s\to\tau\nu)_{\text{SM}} = (5.40\pm0.30)\%$; $\mathcal{B}(\tau\to K\nu)_{\text{exp}} = (6.96\pm0.10)\times 10^{-3}$ [77], $\mathcal{B}(\tau\to K\nu)_{\text{SM}} = (7.15\pm 0.026)\times 10^{-3}$ [56].

3.3 Constraints from the loop-level processes

First of all, the most important one-loop constraint comes from $B_s - \bar{B}_s$ mixing, which is governed by

$$\mathcal{L}_{\text{eff}} = (C_{B_s}^{\text{SM}} + C_{B_s}^{\text{NP}})(\bar{s}\gamma_\mu P_L b)(\bar{s}\gamma^\mu P_L b) + \text{H.c.}, \tag{40}$$

where the SM and NP Wilson coefficients are given respectively by

$$C_{B_s}^{\text{SM}} = -\frac{1}{4\pi^2}G_F^2 m_W^2 \eta_t^2 S(x_t), \tag{41}$$

$$C_{B_s}^{\text{NP}} = -\frac{1}{128\pi^2}\left[\frac{(\lambda'_{i33}\lambda'^*_{i23})^2}{m_{\tilde{b}_R}^2} + \frac{(\lambda'_{233}\lambda'^*_{223})^2}{m_{\tilde{\nu}_\mu}^2}\right], \tag{42}$$

where loop function $S(x_t) = \frac{x_t(4-11x_t+x_t^2)}{4(x_t-1)^2} + \frac{3x_t^3\log(x_t)}{2(x_t-1)^3}$. At 2σ level, the UT*fit* collaboration [81] gives the bound $0.93 < |1 + C_{B_s}^{\text{NP}}/C_{B_s}^{\text{SM}}| < 1.29$.

Next, we investigate a series of Z decaying to two charged leptons with the same flavour like $Z \to \mu\mu(\tau\tau)$ and the different one like $Z\to\mu\tau$. The amplitude of these diagrams is $i\mathcal{M} = i\frac{g}{32\pi^2\cos\theta_W}B_{ij}\epsilon^\alpha\bar{u}_{\ell_i}\gamma_\alpha P_L v_{\ell_j}$ [50], where $B_{ij} = B_{ij}^1 + B_{ij}^2$ and [50,82]

$$B_{ij}^1 = \sum_{l=1}^{2}\tilde{\lambda}'_{jl3}\tilde{\lambda}'^*_{il3}\frac{m_Z^2}{m_{\tilde{b}_R}^2}\left[\left(1-\frac{4}{3}\sin^2\theta_W\right)\right.$$

$$\left.\times\left(\log\frac{m_Z^2}{m_{\tilde{b}_R}^2} - i\pi - \frac{1}{3}\right) + \frac{\sin^2\theta_W}{9}\right], \tag{43}$$

$$B_{ij}^2 = 3\tilde{\lambda}'_{j33}\tilde{\lambda}'^*_{i33}\left\{-x_{\tilde{b}_R}(1+\log x_{\tilde{b}_R})\right.$$
$$+\frac{m_Z^2}{18m_{\tilde{b}_R}^2}\left[(11-10\sin^2\theta_W)+(6-8\sin^2\theta_W)\log x_{\tilde{b}_R}\right.$$
$$\left.\left.+\frac{1}{10}(-9+16\sin^2\theta_W)\frac{m_Z^2}{m_t^2}\right]\right\}, \tag{44}$$

here B_{ij}^1 is the contribution from the diagram induced by exchanging $\tilde{b}_R - u - u$ or $\tilde{b}_R - c - c$ in triangular loop and B_{ij}^2 is the contribution from the diagram induced by exchanging $\tilde{b}_R - t - t$ in triangular loop. As shown in Ref. [50], for $Z\to\mu\mu(\tau\tau)$, demanding the interference term in the partial width between the SM tree-level contribution and the NP one-loop level ones is less than twice the experimental uncertainty on the partial width [77], there are the bounds $|\Re(B_{22})| < 0.32$ and $|\Re(B_{33})| < 0.39$ [50]. And the experimental upper limit $\mathcal{B}(Z\to\mu\tau) < 1.2\times 10^{-5}$ [77] makes the bound $\sqrt{|B_{23}|^2 + |B_{32}|^2} < 2.1$ [50].

Finally, we discuss the lepton-flavour violating decay of τ lepton, including $\tau\to\mu\gamma$ and $\tau\to\mu\mu\mu$. In the limit $m_\mu^2/m_\tau^2 \to 0$, the branching fraction for $\tau\to\mu\gamma$ is given by [68,83,84]

$$\mathcal{B}(\tau\to\mu\gamma) = \frac{\tau_\tau\alpha m_\tau^5}{4}(|A_2^L|^2 + |A_2^R|^2), \tag{45}$$

where the effective couplings $A_2^{L,R}$ come from on shell photon penguin diagrams [68],

$$A_2^L = -\frac{\lambda'_{2j3}\lambda'^*_{3j3}}{64\pi^2 m_{\tilde{b}_R}^2}, \quad A_2^R = 0. \tag{46}$$

The current experimental upper limit is $\mathcal{B}(\tau\to\mu\gamma) < 4.4\times 10^{-8}$ at 90% CL [77].

In general, the effective Lagrangian leading to $\tau\to\mu\mu\mu$ decay is given by [83,84]

$$\mathcal{L}_{\text{eff}} = -\frac{B_1}{2}(\bar{\tau}\gamma^\nu P_L\mu)(\bar{\mu}\gamma_\nu P_R\mu) - \frac{B_2}{2}(\bar{\tau}\gamma^\nu P_R\mu)(\bar{\mu}\gamma_\nu P_L\mu)$$
$$+ C_1(\bar{\tau}P_R\mu)(\bar{\mu}P_R\mu) + C_2(\bar{\tau}P_L\mu)(\bar{\mu}P_L\mu)$$
$$+ G_1(\bar{\tau}\gamma^\nu P_R\mu)(\bar{\mu}\gamma_\nu P_R\mu) + G_2(\bar{\tau}\gamma^\nu P_L\mu)(\bar{\mu}\gamma_\nu P_L\mu)$$

$$- A_R(\bar{\tau}[\gamma_\mu, \gamma_\nu]\frac{q^\nu}{q^2}P_R\mu)(\bar{\mu}\gamma^\mu\mu)$$
$$- A_L(\bar{\tau}[\gamma_\mu, \gamma_\nu]\frac{q^\nu}{q^2}P_L\mu)(\bar{\mu}\gamma^\mu\mu) + \text{H.c.}. \quad (47)$$

This Lagrangian leads to [83,84]

$$\mathcal{B}(\tau \to 3\mu) = \frac{\tau_\tau m_\tau^5}{6144\pi^3}\Bigg[|B_1|^2 + |B_2|^2 + 8(|G_1|^2 + |G_2|^2) + \frac{|C_1|^2 + |C_2|^2}{2} + 32\left(4\log\frac{m_\tau^2}{m_\mu^2} - 11\right)\frac{|A_R|^2 + |A_L|^2}{m_\tau^2} - 64\frac{\Re(A_L G_2^* + A_R G_1^*)}{m_\tau} + 32\frac{\Re(A_L B_1^* + A_R B_2^*)}{m_\tau}\Bigg]. \quad (48)$$

In our scenario, there are three different types of contributions, the photonic and Z penguins as well as box diagrams with four λ' couplings, that can contribute to $\tau \to \mu\mu\mu$ decay. The nonzero Wilson coefficients are [50,68]

$$B_1 = -2\big(4\pi\alpha A_1^L + \sin^2\theta_W B'\big), \quad (49)$$

$$G_2 = 4\pi\alpha A_1^L + \left(-\frac{1}{2} + \sin^2\theta_W\right)B' + C_\tau, \quad (50)$$

$$A_L = 2\pi\alpha m_\tau A_2^L, \quad (51)$$

where

$$B' = -\frac{3\alpha\tilde{\lambda}'_{233}\tilde{\lambda}'^*_{333}x_{\tilde{b}_R}(1 + \log x_{\tilde{b}_R})}{8\pi\cos^2\theta_W\sin^2\theta_W m_Z^2}, \quad (52)$$

$$C_\tau = \frac{i}{4}\tilde{\lambda}'_{2i3}\tilde{\lambda}'^*_{2i3}\tilde{\lambda}'_{2j3}\tilde{\lambda}'^*_{3j3}D_2[m_{\tilde{b}_R}^2, m_{\tilde{b}_R}^2, m_{u_i}^2, m_{u_j}^2], \quad (53)$$

and the off-shell effective coupling A_1^L is [68]

$$A_1^L = \frac{\lambda'_{2j3}\lambda'^*_{3j3}}{16\pi^2 m_{\tilde{b}_R}^2}\left[\frac{1}{18} - \frac{2}{3}\left(\frac{4}{3} + \log\frac{m_{u_j}^2}{m_{\tilde{b}_R}^2}\right)\right]. \quad (54)$$

The current experimental upper limit on the branching fraction for this decay is $\mathcal{B}(\tau \to \mu\mu\mu) < 2.1 \times 10^{-8}$ at 90% CL [77].

4 Numerical results and discussions

In this section, we discuss how to interpret both $b \to s\ell^+\ell^-$ and $R(D^{(*)})$ anomalies and satisfy all these potential constraints simultaneously. The relevant model parameters in our scenario are the wino mass $m_{\tilde{W}}$, the mass of muon sneutrino $m_{\tilde{\nu}_\mu}$, the mass of right-handed sbottom $m_{\tilde{b}_R}$, as well as four nonzero couplings λ'_{223}, λ'_{233}, λ'_{323}, and λ'_{333}. We set $m_{\tilde{W}} = 250$ GeV. It can be seen from Ref. [52] that a positive product $\lambda'_{233}\lambda'^*_{223}$ is needed to explain the $b \to s\ell^+\ell^-$ anomaly mainly through muon sneutrinos (the C_9^{V} part). Both λ'_{323} and λ'_{333} are positive to help solve $R(D^{(*)})$ anomaly by exchanging $\tilde{b}_R$ at tree level [56]. The combination of the choice of above couplings will naturally produce a negative C_9^{U}, which is in line with the conclusion of the global analysis [20]. Our numerical results are shown in Fig. 3. These results show that it is possible to explain $b \to s\ell^+\ell^-$ and $R(D^{(*)})$ anomalies simultaneously at 2σ level.[4] The regions of NP parameters that can solve B-physics anomalies are most constrained by $B \to K^{(*)}\nu\bar{\nu}$ decays, $B_s - \bar{B}_s$ mixing and Z decays. In addition, the $\tau \to \mu\mu\mu$ decay can provide a weak constraint. We find that other related processes, such as $D^0 \to \mu^+\mu^-$, $\tau \to \mu\rho^0$, $B \to \tau\nu$, $D_s \to \tau\nu$, $\tau \to K\nu$, and $\tau \to \mu\gamma$ decays, do not provide available constraints.

We show in Fig. 3a, b the allowed regions in the planes of coupling parameters (λ'_{233}, λ'_{333}) and (λ'_{223}, λ'_{323}) respectively when other parameters are fixed. These two subfigures show that in order to explain the B-physics anomalies, the coupling parameters need to satisfy the relation $\lambda'_{333} > \lambda'_{233} > \lambda'_{323} \simeq \lambda'_{223}$, and the required λ'_{223} and λ'_{323} are very small. Therefore, the next four subfigures in Fig. 3 mainly discuss the relationships between the coupling parameters λ'_{333} and λ'_{233} and the masses $m_{\tilde{b}_R}$ and $m_{\tilde{\nu}_\mu}$. From Fig. 3a, we can see that λ'_{333} is more constrained by $R(D^{(*)})$, $B \to K^{(*)}\nu\bar{\nu}$ and Z decays, but less affected by $b \to s\ell^+\ell^-$ processes and $B_s - \bar{B}_s$ mixing. On the contrary, λ'_{233} is greatly constrained by $b \to s\ell^+\ell^-$ processes and $B_s - \bar{B}_s$ mixing, but has little influence on $R(D^{(*)})$, $B \to K^{(*)}\nu\bar{\nu}$ and Z decays. As shown in Fig. 3c, after the variable parameter $m_{\tilde{b}_R}$ is added, the constraints of λ'_{333} from $R(D^{(*)})$, $B \to K^{(*)}\nu\bar{\nu}$ and Z decays will be relaxed a lot. The parameters λ'_{333} and $m_{\tilde{b}_R}$ are highly correlated. Because we choose a smaller mass of muon sneutrino, the $B_s - \bar{B}_s$ mixing is more sensitive to $m_{\tilde{\nu}_\mu}$ than to $m_{\tilde{b}_R}$, which can be seen by comparing Fig. 3d with Fig. 3f. All subfigures contain parameter spaces (marked in purple) that can resolve $b \to s\ell^+\ell^-$ and $R(D^{(*)})$ anomalies, and satisfy the constraints from other related processes simultaneously.

5 Conclusions

The recent measurements on semileptonic decays of B-meson suggest the existence of NP which breaks the LFU. Among them, the observables $R_{K^{(*)}}$ and P_5' in $b \to s\ell^+\ell^-$ processes and the $R(D^{(*)})$ in $B \to D^{(*)}\tau\nu$ decays are more striking. They are collectively called B-physics anomalies.

[4] In order to consider the constraints from $B \to K^{(*)}\nu\bar{\nu}$, $\tau \to \mu\gamma$ and $\tau \to \mu\mu\mu$ decays at 2σ level, we get the experimental bounds (assuming the uncertainties follow the Gaussian distribution [85]) $R_{23}^{\nu\bar{\nu}} < 3.3$, $\mathcal{B}(\tau \to \mu\gamma) < 5.4 \times 10^{-8}$ and $\mathcal{B}(\tau \to \mu\mu\mu) < 2.6 \times 10^{-8}$, respectively.

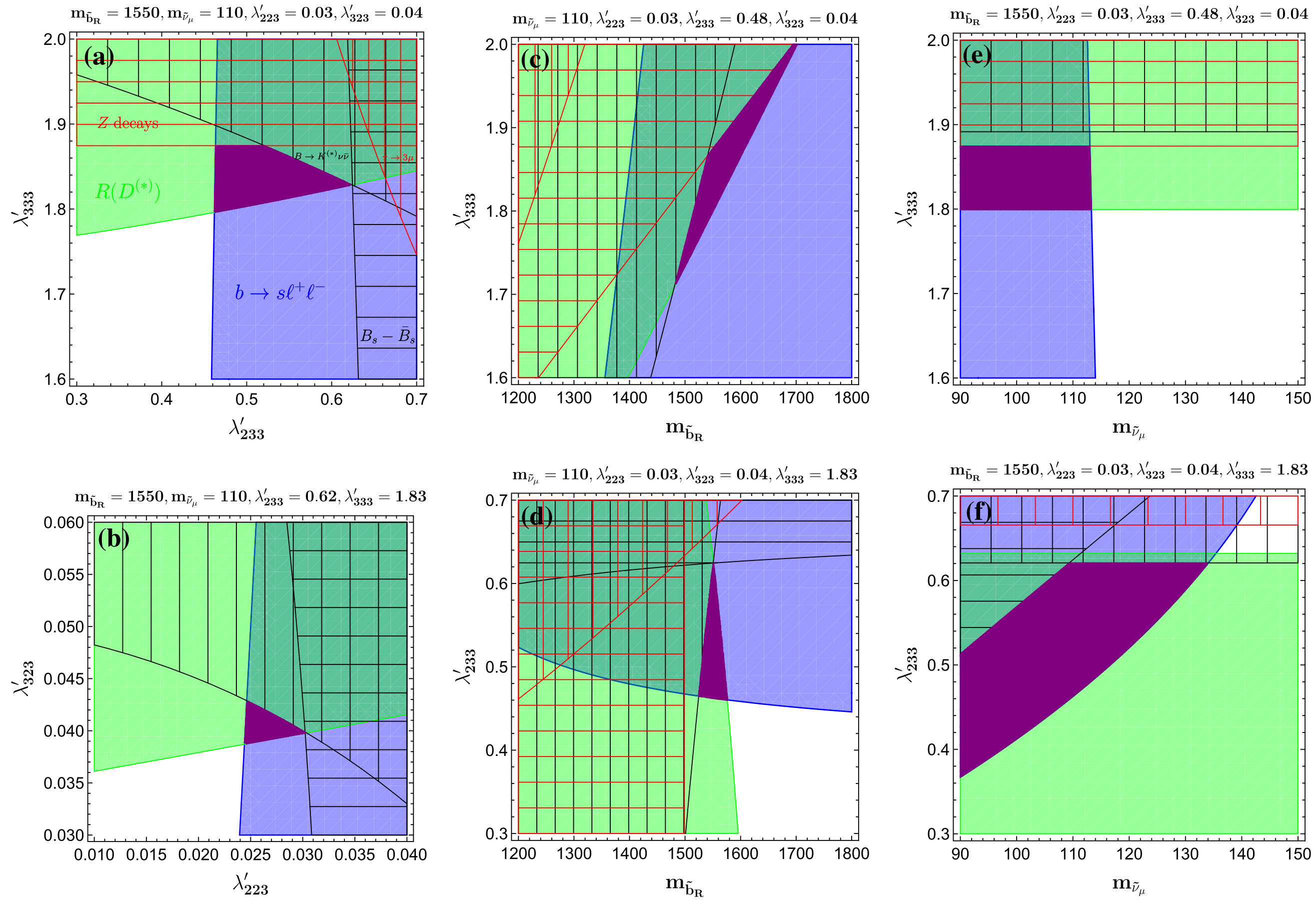

Fig. 3 Numerical analysis in which $b \to s\ell^+\ell^-$ and $R(D^{(*)})$ anomalies are solved and other constraints are satisfied. The masses $m_{\tilde{b}_R}$ and $m_{\tilde{\nu}_\mu}$ are given in units of GeV. The 2σ favored regions from the $b \to s\ell^+\ell^-$ and $R(D^{(*)})$ measurements are shown in blue and green, respectively. The hatched areas filled with black-vertical, black-horizontal, red-horizontal, and red-vertical lines are excluded by $B \to K^{(*)}\nu\bar{\nu}$ decays, $B_s - \bar{B}_s$ mixing, Z decays, and $\tau \to \mu\mu\mu$ decay, respectively. The overlaps are marked in purple

In this work, we have explored the possibility of using muon sneutrinos $\tilde{\nu}_\mu$ and right-handed sbottoms $\tilde{b}_R$ to solve these B-physics anomalies simultaneously in R-parity violating MSSM.

To explain the anomalies in $b \to s\ell^+\ell^-$ processes, we use a two-parameter scenario, where the total Wilson coefficients of NP are divided into two parts, one is the $C_9^{\rm V}$ (Noting $C_{10,\mu}^{\rm NP} = -C_9^{\rm V}$) that only contributes the muon channel and the other is the $C_9^{\rm U}$ that contributes both the electron and the muon channels. First, we scrutinize all the one-loop contributions of the superpotential terms $\lambda'_{ijk} L_i Q_j D_k^c$ to the $b \to s\ell^+\ell^-$ processes under the assumptions $\lambda'_{ij1} = \lambda'_{ij2} = 0$ and $\lambda'_{1j3} = 0$. We find that the contribution from the $H^\pm - \tilde{b}_R$ box diagram (Fig. 1c) is missed in the literature, this contribution is usually positive, and we find that it is numerically negligible when $\tan\beta > 2$. The photonic penguin induced by exchanging sneutrino can provide important contribution due to the existence of logarithmic enhancement, which has never been addressed before. This contribution is lepton flavour universal due to the SM photon, so it is natural to contribute a nonzero $C_9^{\rm U}$.

Global analyses show that the sizable magnitude of $C_9^{\rm V}$ is needed to explain $b \to s\ell^+\ell^-$ anomaly. However, $C_9^{\rm V}$ in the scenario with nonzero $C_9^{\rm U}$ is smaller than the one in the scenario without $C_9^{\rm U}$. With the addition of the latest measurements from the Belle collaboration, the world averages of $R(D^{(*)})$ are closer to the predicted values of the SM. These changes make it possible to use $\tilde{\nu}_\mu$ and $\tilde{b}_R$ to explain $b \to s\ell^+\ell^-$ and $R(D^{(*)})$ anomalies, simultaneously. We also consider the constraints of other related processes in our scenario. The strongest constraints come from $B \to K^{(*)}\nu\bar{\nu}$ decays, $B_s - \bar{B}_s$ mixing, and the processes of Z decays. Besides, $\tau \to \mu\mu\mu$ decay can provide a few constraints. The other decays, such as $D^0 \to \mu^+\mu^-$, $\tau \to \mu\rho^0$, $B \to \tau\nu$, $D_s \to \tau\nu$, $\tau \to K\nu$, and $\tau \to \mu\gamma$, do not provide available constraints.

Acknowledgements This work is supported by the National Natural Science Foundation of China under Grant Nos. 11947083 and 11775092.

Data Availability Statement This manuscript has no associated data or the data will not be deposited. [Authors' comment: All data generated during this study are already contained in this published paper.]

Funded by SCOAP³.

References

1. LHCb collaboration, Search for lepton-universality violation in $B^+ \to K^+\ell^+\ell^-$ decays. Phys. Rev. Lett. **122**, 191801 (2019). https://doi.org/10.1103/PhysRevLett.122.191801. arXiv:1903.09252
2. LHCb collaboration, Test of lepton universality using $B^+ \to K^+\ell^+\ell^-$ decays. Phys. Rev. Lett. **113**, 151601 (2014). https://doi.org/10.1103/PhysRevLett.113.151601. arXiv:1406.6482
3. M. Bordone, G. Isidori, A. Pattori, On the standard model predictions for R_K and R_{K^*}. Eur. Phys. J. C **76**, 440 (2016). https://doi.org/10.1140/epjc/s10052-016-4274-7. arXiv:1605.07633
4. LHCb collaboration, Test of lepton universality with $B^0 \to K^{*0}\ell^+\ell^-$ decays. JHEP **08**, 055 (2017). https://doi.org/10.1007/JHEP08(2017)055. arXiv:1705.05802
5. Belle collaboration, Test of lepton flavor universality in $B \to K\ell^+\ell^-$ decays. arXiv:1908.01848
6. Belle collaboration, Test of lepton flavor universality in $B \to K^*\ell^+\ell^-$ decays at Belle. arXiv:1904.02440
7. S. Descotes-Genon, J. Matias, M. Ramon, J. Virto, Implications from clean observables for the binned analysis of $B \to K^*\mu^+\mu^-$ at large recoil. JHEP **01**, 048 (2013). https://doi.org/10.1007/JHEP01(2013)048. arXiv:1207.2753
8. S. Descotes-Genon, T. Hurth, J. Matias, J. Virto, Optimizing the basis of $B \to K^*ll$ observables in the full kinematic range. JHEP **05**, 137 (2013). https://doi.org/10.1007/JHEP05(2013)137. arXiv:1303.5794
9. Q.-Y. Hu, X.-Q. Li, Y.-D. Yang, $B^0 \to K^{*0}\mu^+\mu^-$ decay in the aligned two-higgs-doublet model. Eur. Phys. J. C **77**, 190 (2017). https://doi.org/10.1140/epjc/s10052-017-4748-2. arXiv:1612.08867
10. LHCb collaboration, Angular analysis of the $B^0 \to K^{*0}\mu^+\mu^-$ decay using 3 fb^{-1} of integrated luminosity. JHEP **02**, 104 (2016). https://doi.org/10.1007/JHEP02(2016)104. arXiv:1512.04442
11. LHCb collaboration, Measurement of Form-Factor-Independent Observables in the Decay $B^0 \to K^{*0}\mu^+\mu^-$. Phys. Rev. Lett. **111**, 191801 (2013). https://doi.org/10.1103/PhysRevLett.111.191801. arXiv:1308.1707
12. CMS collaboration, Angular analysis of the decay $B^0 \to K^{*0}\mu^+\mu^-$ from pp collisions at $\sqrt{s} = 8$ TeV. Phys. Lett. B **753**, 424 (2016). https://doi.org/10.1016/j.physletb.2015.12.020. arXiv:1507.08126
13. ATLAS collaboration, Angular analysis of $B_d^0 \to K^*\mu^+\mu^-$ decays in pp collisions at $\sqrt{s} = 8$ TeV with the ATLAS detector. JHEP **10**, 047 (2018). https://doi.org/10.1007/JHEP10(2018)047. arXiv:1805.04000
14. Belle collaboration, Lepton-Flavor-dependent angular analysis of $B \to K^*\ell^+\ell^-$. Phys. Rev. Lett. **118**, 111801 (2017). https://doi.org/10.1103/PhysRevLett.118.111801. arXiv:1612.05014
15. Belle collaboration, Angular analysis of $B^0 \to K^*(892)^0\ell^+\ell^-$. arXiv:1604.04042
16. LHCb collaboration, Angular analysis and differential branching fraction of the decay $B_s^0 \to \phi\mu^+\mu^-$. JHEP **09**, 179 (2015). https://doi.org/10.1007/JHEP09(2015)179. arXiv:1506.08777
17. LHCb collaboration, Differential branching fraction and angular analysis of the decay $B_s^0 \to \phi\mu^+\mu^-$. JHEP **07**, 084 (2013). https://doi.org/10.1007/JHEP07(2013)084. arXiv:1305.2168
18. J. Aebischer, W. Altmannshofer, D. Guadagnoli, M. Reboud, P. Stangl, D. M. Straub, B-decay discrepancies after Moriond 2019. arXiv:1903.10434
19. A.K. Alok, A. Dighe, S. Gangal, D. Kumar, Continuing search for new physics in $b \to s\mu\mu$ decays: two operators at a time. JHEP **06**, 089 (2019). https://doi.org/10.1007/JHEP06(2019)089. arXiv:1903.09617
20. M. Algueró, B. Capdevila, A. Crivellin, S. Descotes-Genon, P. Masjuan, J. Matias et al., Emerging patterns of new physics with and without lepton flavour universal contributions. Eur. Phys. J. C **79**, 714 (2019). https://doi.org/10.1140/epjc/s10052-019-7216-3. arXiv:1903.09578
21. M. Ciuchini, A.M. Coutinho, M. Fedele, E. Franco, A. Paul, L. Silvestrini et al., New physics in $b \to s\ell^+\ell^-$ confronts new data on Lepton Universality. Eur. Phys. J. C **79**, 719 (2019). https://doi.org/10.1140/epjc/s10052-019-7210-9. arXiv:1903.09632
22. A. Arbey, T. Hurth, F. Mahmoudi, D.M. Santos, S. Neshatpour, Update on the $b \to s$ anomalies. Phys. Rev. D **100**, 015045 (2019). https://doi.org/10.1103/PhysRevD.100.015045. arXiv:1904.08399
23. K. Kowalska, D. Kumar, E.M. Sessolo, Implications for new physics in $b \to s\mu\mu$ transitions after recent measurements by Belle and LHCb. Eur. Phys. J. C **79**, 840 (2019). https://doi.org/10.1140/epjc/s10052-019-7330-2. arXiv:1903.10932
24. B. Capdevila, U. Laa, G. Valencia, Fitting in or odd one out? Pulls vs residual responses in $b \to s\ell^+\ell^-$. arXiv:1908.03338
25. S. Bhattacharya, A. Biswas, S. Nandi, S.K. Patra, Exhaustive Model Selection in $b \to s\ell\ell$ Decays: pitting cross-validation against AIC$_c$. arXiv:1908.04835
26. M. Algueró, B. Capdevila, S. Descotes-Genon, P. Masjuan, J. Matias, Are we overlooking lepton flavour universal new physics in $b \to s\ell\ell$? Phys. Rev. D **99**, 075017 (2019). https://doi.org/10.1103/PhysRevD.99.075017. arXiv:1809.08447
27. R. Barbier et al., R-parity violating supersymmetry. Phys. Rep. **420**, 1 (2005). https://doi.org/10.1016/j.physrep.2005.08.006. arXiv:hep-ph/0406039
28. BaBar collaboration, Evidence for an excess of $\bar{B} \to D^{(*)}\tau^-\bar{\nu}_\tau$ decays. Phys. Rev. Lett. **109**, 101802 (2012). https://doi.org/10.1103/PhysRevLett.109.101802. arXiv:1205.5442
29. BaBar collaboration, Measurement of an Excess of $\bar{B} \to D^{(*)}\tau^-\bar{\nu}_\tau$ decays and implications for charged Higgs bosons. Phys. Rev. D **88**, 072012 (2013). https://doi.org/10.1103/PhysRevD.88.072012. arXiv:1303.0571
30. Belle collaboration, Measurement of the branching ratio of $\bar{B} \to D^{(*)}\tau^-\bar{\nu}_\tau$ relative to $\bar{B} \to D^{(*)}\ell^-\bar{\nu}_\ell$ decays with hadronic tagging at Belle. Phys. Rev. D **92**, 072014 (2015). https://doi.org/10.1103/PhysRevD.92.072014. arXiv:1507.03233
31. Belle collaboration, Measurement of $\mathcal{R}(D)$ and $\mathcal{R}(D^*)$ with a semileptonic tagging method. arXiv:1910.05864

32. BELLE collaboration, Measurement of the τ lepton polarization and $R(D^*)$ in the decay $\bar{B} \to D^*\tau^-\bar{\nu}_\tau$. Phys. Rev. Lett. **118**, 211801 (2017). https://doi.org/10.1103/PhysRevLett.118.211801. arXiv:1612.00529
33. BELLE collaboration, Measurement of the τ lepton polarization and $R(D^*)$ in the decay $\bar{B} \to D^*\tau^-\bar{\nu}_\tau$ with one-prong hadronic τ decays at Belle. Phys. Rev. D **97**, 012004 (2018). https://doi.org/10.1103/PhysRevD.97.012004. arXiv:1709.00129
34. LHCB collaboration, Measurement of the ratio of branching fractions $\mathcal{B}(\bar{B}^0 \to D^{*+}\tau^-\bar{\nu}_\tau)/\mathcal{B}(\bar{B}^0 \to D^{*+}\mu^-\bar{\nu}_\mu)$. Phys. Rev. Lett. **115**, 111803 (2015). https://doi.org/10.1103/PhysRevLett.115.159901. https://doi.org/10.1103/PhysRevLett.115.111803. arXiv:1506.08614
35. LHCB collaboration, Measurement of the ratio of the $B^0 \to D^{*-}\tau^+\nu_\tau$ and $B^0 \to D^{*-}\mu^+\nu_\mu$ branching fractions using three-prong τ-lepton decays. Phys. Rev. Lett. **120**, 171802 (2018). https://doi.org/10.1103/PhysRevLett.120.171802. arXiv:1708.08856
36. LHCB collaboration, Test of Lepton Flavor Universality by the measurement of the $B^0 \to D^{*-}\tau^+\nu_\tau$ branching fraction using three-prong τ decays. Phys. Rev. D **97**, 072013 (2018). https://doi.org/10.1103/PhysRevD.97.072013. arXiv:1711.02505
37. HFLAV collaboration, Averages of b-hadron, c-hadron, and τ-lepton properties as of 2018. arXiv:1909.12524
38. HFLAV collaboration, Online update for averages of R_D and R_{D^*} for Spring 2019 at https://hflav-eos.web.cern.ch/hflav-eos/semi/spring19/html/RDsDsstar/RDRDs.html
39. D. Bigi, P. Gambino, Revisiting $B \to D\ell\nu$. Phys. Rev. D **94**, 094008 (2016). https://doi.org/10.1103/PhysRevD.94.094008. arXiv:1606.08030
40. F.U. Bernlochner, Z. Ligeti, M. Papucci, D.J. Robinson, Combined analysis of semileptonic B decays to D and D^*: $R(D^{(*)})$, $|V_{cb}|$, and new physics. Phys. Rev. D **95**, 115008 (2017). https://doi.org/10.1103/PhysRevD.95.115008. https://doi.org/10.1103/PhysRevD.97.059902. arXiv:1703.05330
41. D. Bigi, P. Gambino, S. Schacht, $R(D^*)$, $|V_{cb}|$, and the heavy quark symmetry relations between form factors. JHEP **11**, 061 (2017). https://doi.org/10.1007/JHEP11(2017)061. arXiv:1707.09509
42. S. Jaiswal, S. Nandi, S.K. Patra, Extraction of $|V_{cb}|$ from $B \to D^{(*)}\ell\nu_\ell$ and the Standard Model predictions of $R(D^{(*)})$. JHEP **12**, 060 (2017). https://doi.org/10.1007/JHEP12(2017)060. arXiv:1707.09977
43. Q.-Y. Hu, X.-Q. Li, Y.-D. Yang, $b \to c\tau\nu$ transitions in the standard model effective field theory. Eur. Phys. J. C **79**, 264 (2019). https://doi.org/10.1140/epjc/s10052-019-6766-8. arXiv:1810.04939
44. A.K. Alok, D. Kumar, S. Kumbhakar, S. Uma Sankar, Solutions to R_D-R_{D^*} in light of Belle 2019 data. Nucl. Phys. B **953**, 114957 (2020). https://doi.org/10.1016/j.nuclphysb.2020.114957. arXiv:1903.10486
45. C. Murgui, A. Peñuelas, M. Jung, A. Pich, Global fit to $b \to c\tau\nu$ transitions. JHEP **09**, 103 (2019). https://doi.org/10.1007/JHEP09(2019)103. arXiv:1904.09311
46. R.-X. Shi, L.-S. Geng, B. Grinstein, S. Jäger, J. Martin Camalich, Revisiting the new-physics interpretation of the $b \to c\tau\nu$ data. JHEP **12**, 065 (2019). https://doi.org/10.1007/JHEP12(2019)065. arXiv:1905.08498
47. K. Cheung, Z.-R. Huang, H.-D. Li, C.-D. Lü, Y.-N. Mao, R.-Y. Tang, Revisit to the $b \to c\tau\nu$ transition: in and beyond the SM. arXiv:2002.07272
48. S. Biswas, D. Chowdhury, S. Han, S.J. Lee, Explaining the lepton non-universality at the LHCb and CMS within a unified framework. JHEP **02**, 142 (2015). https://doi.org/10.1007/JHEP02(2015)142. arXiv:1409.0882
49. D. Das, C. Hati, G. Kumar, N. Mahajan, Scrutinizing R-parity violating interactions in light of $R_{K^{(*)}}$ data. Phys. Rev. D **96**, 095033 (2017). https://doi.org/10.1103/PhysRevD.96.095033. arXiv:1705.09188
50. K. Earl, T. Grégoire, Contributions to $b \to s\ell\ell$ anomalies from R-parity violating interactions. JHEP **08**, 201 (2018). https://doi.org/10.1007/JHEP08(2018)201. arXiv:1806.01343
51. L. Darmé, K. Kowalska, L. Roszkowski, E.M. Sessolo, Flavor anomalies and dark matter in SUSY with an extra U(1). JHEP **10**, 052 (2018). https://doi.org/10.1007/JHEP10(2018)052. arXiv:1806.06036
52. Q.-Y. Hu, L.-L. Huang, Explaining $b \to s\ell^+\ell^-$ data by sneutrinos in the R-parity violating MSSM. Phys. Rev. D **101**, 035030 (2020). https://doi.org/10.1103/PhysRevD.101.035030. arXiv:1912.03676
53. N.G. Deshpande, A. Menon, Hints of R-parity violation in B decays into $\tau\nu$. JHEP **01**, 025 (2013). https://doi.org/10.1007/JHEP01(2013)025. arXiv:1208.4134
54. J. Zhu, H.-M. Gan, R.-M. Wang, Y.-Y. Fan, Q. Chang, Y.-G. Xu, Probing the R-parity violating supersymmetric effects in the exclusive $b \to c\ell^-\bar{\nu}_\ell$ decays. Phys. Rev. D **93**, 094023 (2016). https://doi.org/10.1103/PhysRevD.93.094023. arXiv:1602.06491
55. W. Altmannshofer, P.S. Bhupal Dev, A. Soni, $R_{D^{(*)}}$ anomaly: a possible hint for natural supersymmetry with R-parity violation. Phys. Rev. D **96**, 095010 (2017). https://doi.org/10.1103/PhysRevD.96.095010. arXiv:1704.06659
56. Q.-Y. Hu, X.-Q. Li, Y. Muramatsu, Y.-D. Yang, R-parity violating solutions to the $R_{D^{(*)}}$ anomaly and their GUT-scale unifications. Phys. Rev. D **99**, 015008 (2019). https://doi.org/10.1103/PhysRevD.99.015008. arXiv:1808.01419
57. D.-Y. Wang, Y.-D. Yang, X.-B. Yuan, $b \to c\tau\bar{\nu}$ decays in supersymmetry with R-parity violation. Chin. Phys. C **43**, 083103 (2019). https://doi.org/10.1088/1674-1137/43/8/083103. arXiv:1905.08784
58. N.G. Deshpande, X.-G. He, Consequences of R-parity violating interactions for anomalies in $\bar{B} \to D^{(*)}\tau\bar{\nu}$ and $b \to s\mu^+\mu^-$. Eur. Phys. J. C **77**, 134 (2017). https://doi.org/10.1140/epjc/s10052-017-4707-y. arXiv:1608.04817
59. S. Trifinopoulos, Revisiting R-parity violating interactions as an explanation of the B-physics anomalies. Eur. Phys. J. C **78**, 803 (2018). https://doi.org/10.1140/epjc/s10052-018-6280-4. arXiv:1807.01638
60. S. Trifinopoulos, B-physics anomalies: the bridge between R-parity violating supersymmetry and flavored dark matter. Phys. Rev. D **100**, 115022 (2019). https://doi.org/10.1103/PhysRevD.100.115022. arXiv:1904.12940
61. M. Bauer, M. Neubert, Minimal leptoquark explanation for the $\mathrm{R}_{D^{(*)}}$, R_K, and $(g-2)_\mu$ anomalies. Phys. Rev. Lett. **116**, 141802 (2016). https://doi.org/10.1103/PhysRevLett.116.141802. arXiv:1511.01900
62. CDF collaboration, Search for R-parity Violating Decays of τ Sneutrinos to $e\mu$, $\mu\tau$, and $e\tau$ Pairs in $p\bar{p}$ Collisions at $\sqrt{s} = 1.96$ TeV. Phys. Rev. Lett. **105**, 191801 (2010). https://doi.org/10.1103/PhysRevLett.105.191801. arXiv:1004.3042
63. D0 collaboration, Search for sneutrino Production in $e\mu$ Final States in 5.3 fb^{-1} of $p\bar{p}$ Collisions at $\sqrt{s}$ =1.96 TeV. Phys. Rev. Lett. **105**, 191802 (2010). https://doi.org/10.1103/PhysRevLett.105.191802. arXiv:1007.4835
64. ATLAS collaboration, Search for a heavy neutral particle decaying to $e\mu$, $e\tau$, or $\mu\tau$ in pp collisions at $\sqrt{s} = 8$ TeV with the ATLAS detector. Phys. Rev. Lett. **115**, 031801 (2015). https://doi.org/10.1103/PhysRevLett.115.031801. arXiv:1503.04430
65. CMS collaboration, Search for lepton flavour violating decays of heavy resonances and quantum black holes to an $e\mu$ pair in proton–proton collisions at $\sqrt{s} = 8$ TeV. Eur. Phys. J. C **76**, 317 (2016). https://doi.org/10.1140/epjc/s10052-016-4149-y. arXiv:1604.05239
66. W. Altmannshofer, D.M. Straub, New physics in $b \to s$ transitions after LHC run 1. Eur. Phys. J. C **75**, 382 (2015). https://doi.org/10.1140/epjc/s10052-015-3602-7. arXiv:1411.3161

67. G. Passarino, M.J.G. Veltman, One loop corrections for e^+e^- annihilation into $\mu^+\mu^-$ in the Weinberg model. Nucl. Phys. B **160**, 151 (1979). https://doi.org/10.1016/0550-3213(79)90234-7
68. A. de Gouvea, S. Lola, K. Tobe, Lepton flavor violation in supersymmetric models with trilinear R-parity violation. Phys. Rev. D **63**, 035004 (2001). https://doi.org/10.1103/PhysRevD.63.035004. arXiv:hep-ph/0008085
69. D. Das, C. Hati, G. Kumar, N. Mahajan, Towards a unified explanation of $R_{D^{(*)}}$, R_K and $(g-2)_\mu$ anomalies in a left-right model with leptoquarks. Phys. Rev. D **94**, 055034 (2016). https://doi.org/10.1103/PhysRevD.94.055034. arXiv:1605.06313
70. E. Kpatcha, I. Lara, D. E. López-Fogliani, C. Muñoz, Explaining muon $g-2$ data in the $\mu\nu$SSM. arXiv:1912.04163
71. A.J. Buras, J. Girrbach-Noe, C. Niehoff, D.M. Straub, $B \to K^{(*)}\nu\overline{\nu}$ decays in the standard model and beyond. JHEP **02**, 184 (2015). https://doi.org/10.1007/JHEP02(2015)184. arXiv:1409.4557
72. Belle collaboration, Search for $\boldsymbol{B \to h\nu\bar{\nu}}$ decays with semileptonic tagging at Belle. Phys. Rev. D **96**, 091101 (2017). https://doi.org/10.1103/PhysRevD.97.099902. https://doi.org/10.1103/PhysRevD.96.091101. arXiv:1702.03224
73. BaBar collaboration, Search for $B \to K^{(*)}\nu\overline{\nu}$ and invisible quarkonium decays. Phys. Rev. D **87**, 112005 (2013). https://doi.org/10.1103/PhysRevD.87.112005. arXiv:1303.7465
74. Belle collaboration, Search for $B \to h^{(*)}\nu\bar{\nu}$ with the full Belle $\Upsilon(4S)$ data sample. Phys. Rev. D **87**, 111103 (2013). https://doi.org/10.1103/PhysRevD.87.111103. arXiv:1303.3719
75. D. Du, A.X. El-Khadra, S. Gottlieb, A.S. Kronfeld, J. Laiho, E. Lunghi et al., Phenomenology of semileptonic B-meson decays with form factors from lattice QCD. Phys. Rev. D **93**, 034005 (2016). https://doi.org/10.1103/PhysRevD.93.034005. [arXiv:1510.02349]
76. J. Aebischer, J. Kumar, P. Stangl, D.M. Straub, A global likelihood for precision constraints and flavour anomalies. Eur. Phys. J. C **79**, 509 (2019). https://doi.org/10.1140/epjc/s10052-019-6977-z. arXiv:1810.07698
77. Particle Data Group collaboration, Review of particle physics. Phys. Rev. D **98**, 030001 (2018). https://doi.org/10.1103/PhysRevD.98.030001
78. Flavour Lattice Averaging Group collaboration, FLAG review 2019. Eur. Phys. J. C **80**, 113 (2020). https://doi.org/10.1140/epjc/s10052-019-7354-7. arXiv:1902.08191
79. J.E. Kim, P. Ko, D.-G. Lee, More on R-parity and lepton family number violating couplings from muon(ium) conversion, and tau and pi0 decays. Phys. Rev. D **56**, 100 (1997). https://doi.org/10.1103/PhysRevD.56.100. arXiv:hep-ph/9701381
80. S. Nandi, S. K. Patra, A. Soni, Correlating new physics signals in $B \to D^{(*)}\tau\nu_\tau$ with $B \to \tau\nu_\tau$. arXiv:1605.07191
81. UTfit collaboration, Model-independent constraints on $\Delta F = 2$ operators and the scale of new physics. JHEP **03**, 049 (2008). https://doi.org/10.1088/1126-6708/2008/03/049. arXiv: 0707.0636, updates are available at http://utfit.org/UTfit/WebHome
82. P. Arnan, D. Becirevic, F. Mescia, O. Sumensari, Probing low energy scalar leptoquarks by the leptonic W and Z couplings. JHEP **02**, 109 (2019). https://doi.org/10.1007/JHEP02(2019)109. arXiv:1901.06315
83. Y. Kuno, Y. Okada, Muon decay and physics beyond the standard model. Rev. Mod. Phys. **73**, 151 (2001). https://doi.org/10.1103/RevModPhys.73.151. arXiv:hep-ph/9909265
84. Y. Farzan, S. Najjari, Extracting the CP-violating phases of trilinear R-parity violating couplings from $\mu \to eee$. Phys. Lett. B **690**, 48 (2010). https://doi.org/10.1016/j.physletb.2010.05.005. arXiv:1001.3207
85. D. Buttazzo, A. Greljo, G. Isidori, D. Marzocca, B-physics anomalies: a guide to combined explanations. JHEP **11**, 044 (2017). https://doi.org/10.1007/JHEP11(2017)044. arXiv:1706.07808